

Bulletin of Volcanology

Hydrogen emission from Erebus volcano, Antarctica

--Manuscript Draft--

Manuscript Number:	
Full Title:	Hydrogen emission from Erebus volcano, Antarctica
Article Type:	Research Article
Corresponding Author:	Yves Moussallam University of Cambridge Cambridge, UNITED KINGDOM
Corresponding Author Secondary Information:	
All Authors:	Yves Moussallam Clive Oppenheimer Alessandro Aiuppa Gaetano Giudice Manuel Moussallam Philip Kyle
Abstract:	<p>The continuous measurement of molecular hydrogen (H₂) emissions from passively degassing volcanoes has recently been made possible thanks to the development of electrochemical sensors. We have used this technology to measure H₂, along with SO₂, H₂O, and CO₂, in the gas and aerosol plume emitted from the lava lake of Erebus volcano, Antarctica. The measurements were made at the crater rim between December 2010 and January 2011. Combined with data for the long-term SO₂ emission rate for Erebus, they indicate a mean H₂ flux of 0.03 kg s⁻¹ (2.8 Mg day⁻¹). The observed H₂ content in the plume is consistent with previous estimates of redox conditions in the lava lake (~0.9 log units below the quartz-fayalite-magnetite buffer). These measurements suggest that H₂ does not combust at the surface of the lake, and that H₂ is kinetically inert in the gas/aerosol plume, retaining the signature of the high-temperature chemical equilibrium reached in the lava lake. We also observe a cyclical variation in the H₂/SO₂ ratio with a period of ~10 min. These cycles correspond to oscillatory patterns of surface motion of the lava lake that have been interpreted as signs of a pulsatory magma supply at the top of the magmatic conduit.</p>
Suggested Reviewers:	<p>William Rose Michigan Technological University raman@mtu.edu</p> <p>Hiroshi Shinohara Geological Survey of Japan shinohara-h@aist.go.jp</p> <p>Patrick Allard Institut de physique du globe de Paris pallard@ipgp.fr</p> <p>Tobias Fischer University of New Mexico fischer@unm.edu</p>

1

2 **Hydrogen emission from Erebus volcano, Antarctica**

3

4 Yves Moussallam¹, Clive Oppenheimer¹, Alessandro Aiuppa^{2,3}, Gaetano Giudice³, Manuel5 Moussallam⁴, Philip Kyle⁵

6

7 ¹ Department of Geography, University of Cambridge, Downing Place, Cambridge, CB2 3EN, UK8 ² Dipartimento DiSTeM, Università di Palermo, Via archirafi 36, 90146, Palermo, Italy9 ³ Istituto Nazionale di Geofisica e Vulcanologia, Sezione di Palermo Via La Malfa, 153, 90146 Palermo, Italy10 ⁴ Institut Telecom - Telecom ParisTech - CNRS/LTCI, 37 rue Dareau, 75014 Paris, France11 ⁵ Department of Earth and Environmental Science, New Mexico Institute of Mining and Technology, 801 Leroy

12 Place, Socorro, NM 87801, USA

13

14 Corresponding author: Yves Moussallam; ym286@cam.ac.uk; Tel: 01223 – 333399; Fax: 01223 – 333392

15

16 ***Abstract***

17 The continuous measurement of molecular hydrogen (H₂) emissions from passively degassing

18 volcanoes has recently been made possible thanks to the development of electrochemical

19 sensors. We have used this technology to measure H₂, along with SO₂, H₂O, and CO₂, in the

20 gas and aerosol plume emitted from the phonolite lava lake at Erebus volcano, Antarctica.

21 The measurements were made at the crater rim between December 2010 and January 2011.

22 Combined with data for the long-term SO₂ emission rate for Erebus, they indicate a mean H₂23 flux of 0.03 kg s⁻¹ (2.8 Mg day⁻¹). The observed H₂ content in the plume is consistent with

24 previous estimates of redox conditions in the lava lake (~0.9 log units below the quartz-

25 fayalite-magnetite buffer). These measurements suggest that H₂ does not combust at the
26 surface of the lake, and that H₂ is kinetically inert in the gas/aerosol plume, retaining the
27 signature of the high-temperature chemical equilibrium reached in the lava lake. We also
28 observe a cyclical variation in the H₂/SO₂ ratio with a period of ~10 min. These cycles
29 correspond to oscillatory patterns of surface motion of the lava lake that have been interpreted
30 as signs of a pulsatory magma supply at the top of the magmatic conduit.

31

32 Keywords: Mt Erebus, hydrogen, magma redox conditions, lava lake, magma degassing.

33

34

35 *Introduction*

36 Hydrogen is one of the most abundant trace species in volcanic emissions (Oppenheimer et al.
37 in press) and is an essential participant in key redox reactions that take place in magmatic
38 gases, e.g.:



40 and



42 At Erebus volcano, emissions to the atmosphere result from the sustained supply of gas via
43 the persistently active lava lake and surrounding fumaroles. Gas composition measured in the
44 plume provides important insights into the redox conditions of the lava lake (assuming
45 thermodynamic equilibrium between the gas phase and the melt). Following recent chemical
46 modeling (Burgisser and Scaillet 2007) arguing for an evolution of the oxidation state of an
47 ascending magma, measurement of redox-sensitive volcanic gas species such as hydrogen
48 assumes particular significance.

49
50 The recent development of highly portable and readily deployed multi-species gas sensing
51 systems (Shinohara 2005; Aiuppa et al. 2005; Aiuppa et al. 2006; De Vito et al. 2007) has
52 enabled measurements of volcanic gas ratios for extended periods, in some cases
53 operationally (Aiuppa, Bertagnini, et al. 2010; Aiuppa, Burton, et al. 2010). Such “multi-gas”
54 approaches complement ultraviolet and infrared spectroscopic applications (Oppenheimer
55 2010) to enable measurement of abundances and fluxes of a range of gas species. However,
56 until very recently, there has not been a practical means for extended surveillance of H₂
57 abundance in dilute volcanic plumes. Here we use a “Multi-GAS” instrument incorporating a
58 specific hydrogen sensor to measure H₂ in the plume emitted from the lava lake of Erebus
59 volcano. Erebus is of particular interest because of the emerging evidence for redox change
60 associated with magma ascent (e.g., Oppenheimer et al. 2011; Burgisser et al. in review).
61 Despite challenging conditions at the rim of the summit crater, measurements were possible
62 for several hours per day spanning a week. Our initial aims were to evaluate the performance
63 of this instrument for continuous gas surveillance on Erebus, to assess implications of the
64 measurements for lava lake redox conditions, and to identify any rapid variability in gas
65 composition of the plume.

66

67 *Methodology*

68 The measurements were made between 6 December 2010 and 3 January 2011 using a
69 purpose-built “Multi-GAS” instrument and a commercial CO₂ and H₂O infrared analyser (for
70 intercomparison). The instruments were deployed intermittently at the crater rim of Erebus
71 volcano at a site ~ 220 m vertically above and ~ 150 m horizontally from the active lava lake
72 (Figure 1). The measurements were mostly made at the “Pump Site” situated on the northern

73 rim of the summit crater since this is where prevailing winds tend to carry the plume (Zreda-
74 Gostynska et al. 1997; Ilyinskaya et al. 2010). Both instruments were powered by a 12 V DC
75 battery, which sustained 6–10 h of unattended operation.

76
77 The commercial instrument was a LI-COR[®] LI-840 CO₂ and H₂O analyser. It is a non-
78 dispersive infrared gas analyzer equipped with a dual wavelength, infrared detection system
79 allowing measurements of CO₂ and H₂O gas species in the range of 0–3000 ppmv and 0–80
80 pptv (parts per thousand), respectively. The accuracy was better than 1.5% for both species
81 and cross sensitivity is < 0.1 ppmv CO₂/pptv H₂O for H₂O and <0.0001 pptv H₂O/ppmv CO₂
82 for CO₂.

83
84 The “Multi-GAS” CO₂, H₂, SO₂ sensor consists of a series of electrochemical sensors and a
85 nondispersive infrared (NDIR) sensor through which the sampled gas is circulated (via a
86 miniature 12 V rotary pump) (Aiuppa et al. 2011). The H₂, H₂S and SO₂ sensors produce an
87 electrical current as a response of the target gas entering the electrolyte and oxidizing or
88 reducing the electrode. This current is proportional to the concentration of the target gas in the
89 total gas volume. The electrochemical sensor for SO₂ (City Technology, sensor type 3ST/F)
90 has a calibration range of 0–30 ppmv, an accuracy of ±2%, a repeatability of 1% and a
91 resolution of 0.5 ppmv. The electrochemical sensor for H₂ (City Technology, sensor type
92 3HYT) has a calibration range of 0–500 ppmv, an accuracy of ±5% a repeatability of 2% and a
93 resolution of 2 ppmv. The NDIR CO₂ sensor (model Gascard II) is calibrated for 0–3000
94 ppmv with an accuracy ±2% and a resolution of 0.8 ppmv. In addition to the gas sensors,
95 temperature and relative humidity (RH) sensors (Galltec) are mounted in the instrument,
96 providing a measuring range of 0–100 % RH and an accuracy of ±2%. All sensors were
97 housed inside a weatherproof box, with the ambient air sampled via Teflon tubing connected

98 to a HEPA filter fed through an inlet in the box. The sampled gas was dispersed via an outlet
99 similarly fed through a hole in the case. The sampled gas was heated to ~30°C on its way
100 through the first hose to prevent freezing and other problems related to the low ambient
101 temperatures (below -25°C).

102
103 An on-board data-logger card in the “Multi-GAS” instrument captured measurements at a rate
104 of 0.5 Hz while the LI-840 output was logged at 1 Hz via a netbook PC. Both instruments
105 were always started simultaneously. The Multi-GAS instrument was recalibrated using
106 standard gas mixtures in the laboratory (accurately measured by gas chromatography) before
107 and after the campaign and showed very little drift.

108

109 *Data Processing*

110 Mixing ratios of SO₂, H₂O, CO₂ and H₂ in the gas phase are retrieved (in ppmv) directly from
111 the laboratory-calibrated sensors using the “840-500” software for the LI-840 and in-house
112 software (developed at INGV Palermo) for the multi-gas instrument. The raw data collected
113 by both instruments show a good correlation between all measured species. The good
114 agreement between the CO₂ measurements obtained by the multi-gas instrument and those
115 obtained by the LI-840 furthers our confidence in the accuracy of the multi-gas instrument
116 CO₂ sensor. Response times of the different sensors vary slightly but are all rapid (timescales
117 of seconds to approach maximum reading). **Figure 2** shows an example of a typical dataset,
118 recorded on 27 December 2010.

119

120 In order to convert the raw mixing ratio data into reliable measurements, several processing
121 steps were applied. Firstly, the difference in response time between sensors was corrected so

122 the time-series of volcanic gas ratios matched. Secondly, the sensor signal resulting from
123 cross-sensitivity with other gases was subtracted.

124
125 The differences in response time for the different sensors were corrected by finding the lag
126 times from correlation analysis of the various time series. Laboratory tests were performed
127 using a set of CO gas standards (from 7 to 500 ppmv) circulated through the Multi-gas
128 instrument in order to determine the cross-sensitivity of the hydrogen sensor to other species.
129 CO was a particular concern because of its abundance in the Erebus gas/aerosol plume
130 (Oppenheimer and Kyle 2008). Mixed CO and H₂ gas calibrations were also carried out.
131 These tests revealed a constant but minor 4% cross sensitivity of the H₂ sensor due to the
132 presence of CO. Although we did not have a CO sensor in the Multi-gas instrument, we can
133 estimate CO abundances point-by-point from measured CO₂ abundance and using a CO₂/CO
134 molar ratio of 13 well-constrained by FTIR spectroscopy (Oppenheimer et al. 2009; Ilanko
135 personal communication). At each point 4% of the estimated CO value was subtracted from
136 the H₂ signal to correct for the cross-sensitivity (Figure 3).

137

138 *Results*

139 Useful data were only acquired during favourable winds that resulted in grounding of the
140 plume at the crater rim (figure 1b). We obtained 25 hours of good quality observations at a
141 sample rate of 0.5 Hz over the 180 hours of data collection . The variable weather conditions
142 and delays in stabilising the internal temperature of the “MultiGas” instrument were
143 responsible for the limited collection time. It is worth noting that Strombolian eruptions of the
144 nature occasionally observed at Erebus (Aster et al. 2003; Dibble et al. 2008) did not occur
145 during the acquisition of this dataset – only the “passive” plume emitted from the lava lake

146 was sampled. Figure 4 shows scatter plots for measurements recorded during the last week of
147 December 2010, which offered the best conditions for plume sampling.

148
149 Results from six days of data yield a mean H₂/SO₂ molar ratio between 1.38 and 1.52 (Figure
150 4a) with most days yielding a ratio close to 1.4, and the average ratio for the whole week
151 being 1.44. Scatter plots for the CO₂ and SO₂ measurements yield CO₂/SO₂ molar ratios
152 varying between 36 and 45 (Figure 4b), with the week's average being 40. We neglect the
153 CO₂/SO₂ ratio obtained for 3 January which shows much higher variability which we ascribe
154 to contamination from nearby fumaroles. The intercept of first order linear regression through
155 the scatter plots of H₂ vs. SO₂ and CO₂ vs. SO₂ should correspond to the atmospheric
156 background H₂ and CO₂ abundances, respectively (since ambient SO₂ is very low (less than
157 10 pptv). In fact, we find values for ambient H₂ between 1.06 and 0.42 ppmv and background
158 CO₂ values between 433 and 385. These are both good approximations to expected
159 atmospheric background mixing ratios for the two gases. For instance, measurements from
160 December 2010 at the South Pole weather station (available at <http://www.esrl.noaa.gov/>)
161 indicate atmospheric abundances of 387.5 ppmv for CO₂ and 0.54 ppmv for H₂. This station is
162 the closest Antarctic research station routinely measuring atmospheric gas abundances at
163 altitude (2900 m a.s.l, c.f. the altitude of the Pump Site of ~ 3700 m). A test run using the
164 "Multi-GAS" instrument on 7 December carried out near Lower Erebus Hut (2 km from the
165 crater) also yielded stable H₂ readings of ~0.5 ppmv though CO₂ readings fluctuated with
166 temperature drift during acquisition (CO₂ values oscillated between 400 and 350 ppmv).
167 These estimates of the ambient mixing ratios of the two gases give further confidence in
168 performance of the "Multi-GAS" instrument sensors. While H₂O was being recorded
169 simultaneously by the LICOR and Multi-GASs instruments, rapid changes of the background

170 atmospheric humidity and possible influence of nearby low-temperature fumaroles precluded
171 reliable retrieval of the lava lake plume's water content.

172
173 Further inspection of our dataset reveals small but clear variations in the retrieved gas ratios
174 which appear cyclical. **Figure 5** shows the evolution of the H₂/SO₂ ratio for part of a 10 h run
175 on 3 January 2011 together with the corresponding pseudo-periodogram obtained using a
176 continuous Morlet wavelet transform analysis of the time series. The pseudo-periodogram
177 shows a strong transform modulus with a cycle of 8 to 12 min. Similar pseudo-periodograms
178 have been produced for all the time series for which data are presented in **Figure 4**, and all
179 reveal cycles with periods of 7 to 14 min. In addition, some pseudo-periodograms show
180 weaker signal strength at a shorter period of 3 to 5 min. Pseudo-periodograms were produced
181 for the CO₂/SO₂ ratio time-series and reveal similar periodicities. This periodicity is the more
182 remarkable since it suggests preservation of a source signature despite the passage of the
183 plume within the crater (from the lava lake to the Pump Site). Time series of the SO₂/H₂ and
184 SO₂/CO₂ ratios were constructed using background H₂ and CO₂ atmospheric values
185 determined by the intersection of the linear regression with the H₂ or CO₂-axis for each day
186 (**Figure 4**) except when that intercept was higher than the lowest measured H₂ or CO₂ value,
187 in which case this lowest H₂ or CO₂ value was used as the background.

188

189 ***Discussion***

190 ***Volcanic H₂ contribution to the Antarctic atmosphere***

191 We have estimated the H₂ flux from Erebus volcano using the average SO₂ flux of 0.71 ± 0.3
192 kg s⁻¹ (Sweeney et al. 2008) and the measured H₂/SO₂ ratio. Using dual-wide field of view
193 UV spectroscopy, Boichu et al. (2010) reported an SO₂ flux varying cyclically from 0.17 to

194 $0.89 \pm 0.2 \text{ kg s}^{-1}$. Oppenheimer et al. (2005) measured an average SO₂ flux of $0.86 \pm 0.2 \text{ kg s}^{-1}$
195 by traversing beneath the horizontal plume using a simple ultraviolet spectrometer system,
196 and Sweeney et al. (2008) estimate was a decadal mean SO₂ flux. Using our mean H₂/SO₂
197 ratio of 1.44 (equivalent to a H₂/SO₂ mass ratio of 0.045) we estimate the mean H₂ flux at
198 Erebus volcano as 0.03 kg s^{-1} (2.8 Mg day^{-1}).

199 This estimated H₂ flux from Erebus represents a significant contribution to the local
200 atmospheric chemistry and the single largest recorded point source of H₂ to the Antarctic
201 atmosphere. For context, the global anthropogenic emission of H₂ from the use of fossil fuels
202 is estimated at 5 to 25 Tg a⁻¹ (Novelli et al. 1999). The Erebus source amounts to $\sim 1 \text{ Gg a}^{-1}$ of
203 H₂ corresponding to 0.004 to 0.02 % of the total global anthropogenic emission. For
204 comparison the hydrogen flux at Mt Etna has been estimated at $\sim 0.00065 \text{ Tg a}^{-1}$ (Aiuppa et al.
205 2011). Mount Erebus hydrogen flux is therefore 1.6 time greater than Etna's while its SO₂ flux
206 is 71 time smaller.

207 *Oxidation state of the Erebus lava lake*

208 Based on a mean bulk plume SO₂/H₂O ratio of 0.023 obtained by FTIR spectroscopy
209 (Oppenheimer et al. 2009), we can convert the mean "Multi-GAS"-measured H₂/SO₂ ratio to
210 an H₂/H₂O ratio of 0.033. From this ratio we can calculate the corresponding oxygen fugacity
211 based on the redox reaction in Equation [1] as follows.

212 The equilibrium constant, K, for this reaction is given by $\frac{f_{\text{H}_2} \times (f_{\text{O}_2})^{\frac{1}{2}}}{f_{\text{H}_2\text{O}}}$

213 where $f_{\text{H}_2} = \gamma_{\text{H}_2} \times P_{\text{H}_2}$; $f_{\text{O}_2} = \gamma_{\text{O}_2} \times P_{\text{O}_2}$; $f_{\text{H}_2\text{O}} = \gamma_{\text{H}_2\text{O}} \times P_{\text{H}_2\text{O}}$

214 with $P_i = x_i \times P$

215 and where f_i is the fugacity of the ith species, γ_i the fugacity coefficient of the ith species, P_i is
216 the partial pressure of the ith species, x_i the mole fraction of the ith species and P is the total
217 gas pressure.

218 Which yields: $(f_{O_2})^{1/2} = \frac{K \times f_{H_2O}}{f_{H_2}} = K \frac{\gamma_{H_2O} \times x_{H_2O} \times P}{\gamma_{H_2} \times x_{H_2} \times P}$

219 and therefore $f_{O_2} = \left(K \frac{\gamma_{H_2O} \times x_{H_2O}}{\gamma_{H_2} \times x_{H_2}} \right)^2$

220 At atmospheric pressure, the fugacity of a gas is equal to its partial pressure (assuming ideal
221 behaviour) therefore $\gamma_{H_2O}/\gamma_{H_2} = 1$. The equilibrium constant can be calculated as follows:

222 $K = \exp(-\Delta G/RT)$

223 $\Delta G = \Delta H - T\Delta S$

224 $\Delta H = \int_{T_1}^{T_2} C_p dt$

225 $\Delta S = \int_{T_1}^{T_2} \frac{C_p}{T} dt$

226 Where ΔG is the change in Gibbs' free energy, ΔH the change in enthalpy, and ΔS the change
227 in entropy of the system. C_p is the heat capacity which can be fit by a function of the form: C_p
228 $= a + bT + cT^{-2} + dT^{-0.5}$ with a, b, c and d representing Maier-Kelly coefficients specific for
229 each substance and obtained here from the Supcrt92 software (Johnson et al. 1992). At $T =$
230 1273K (the most widely accepted temperature of the lava lake), $K = 3.72 \cdot 10^{-8}$, the $\log f_{O_2}$ is
231 equivalent to QFM-0.92 (using a H₂/SO₂ ratio of 1.44, and where QFM refers to the quartz-
232 fayalite-magnetite buffer). Using the obtained oxygen fugacity and prior measurements
233 (Oppenheimer et al. 2009), we can recalculate the composition of the Erebus plume to include
234 H₂ and the expected abundance of H₂S (Table 1, first column). Note that, in the Table, H₂S is
235 estimated based on the gas redox properties (calculated using the "Dcompress" software from
236 Burgisser et al. (in review)) though it has not been detected at Erebus despite multiple
237 attempts (Oppenheimer and Kyle 2008).

238 The oxidation state of the phonolite magma in the persistent lava lake of Erebus volcano has
239 been estimated by several techniques. Kelly et al. (Kelly et al. 2008) used mineral chemistry
240 to estimate an oxidation state of $\Delta \log QFM = -0.9$ (using the QUILF program and a
241 temperature of 1000°C). Oppenheimer & Kyle (2008) and Oppenheimer et al. (2011) used the

242 CO₂/CO ratio obtained using FTIR spectroscopy (and the same temperature) to estimate the
243 oxidation state at $\Delta\log\text{QFM} = -0.9$ to -0.88 . Both of these estimates are very similar to our
244 mean $\Delta\log\text{QFM} = -0.92$. It should be noted however that our new estimate of the oxidation
245 state is not entirely independent as we used the SO₂/H₂O ratio previously measured by FTIR
246 spectroscopy in our calculation.

247
248 The presence of H₂ in the volcanic plume suggests that H₂ is not burning at the interface
249 between the lava lake and the atmosphere as has been observed, for instance, at Kīlauea's lava
250 lake (Cruikshank et al. 1973). The correspondence of computed redox conditions for the lava
251 lake also indicates that the H₂ abundance at the crater rim corresponds to the high-temperature
252 equilibrium with the lava lake as hypothesized by Martin et al. (2009), and experimentally
253 verified at Etna by Aiuppa et al. (2011). If any H₂ is oxidizing in the plume (e.g., to form
254 HO_x radicals) it is only in very small amounts.

255 *Periodicity and magma supply to the lake*

256 From the time-series, the H₂/SO₂ molar ratio varies mostly between 1 and 2 for all six days
257 while the CO₂/SO₂ molar ratio varies mostly between 25 and 50. These upper and lower
258 values can be attributed to two end-member compositions associated with a periodic dynamic
259 behavior of the lake (Table 1) recognised in the lava lake surface motion and other gas ratios
260 (Oppenheimer et al. 2009). The terms “top” and “bottom” of the cycle are adopted here to
261 echo previous literature; the “Top of cycle” refers to high SO₂/CO₂ ratio, faster lake motion
262 and higher lake level, and, as shown in Figure 5, corresponds to high SO₂/H₂. The “top of
263 cycle” composition is calculated using an H₂/SO₂ ratio of 1 and SO₂/H₂O gas ratios of 0.0242
264 from the “mixed plume” composition of Oppenheimer et al. (2009) while the “Bottom of
265 cycle” composition is calculated using an H₂/SO₂ ratio of 2 and SO₂/H₂O gas ratios of 0.0218
266 from the “conduit gas” composition of Oppenheimer et al. (2009). The difference between the

267 two end-member compositions is quite significant in term of redox state, representing QFM-
268 0.65 at the “top of the cycle” and QFM-1.16 at the “bottom of the cycle” (assuming no change
269 in temperature).

270 Considering that the “tops” of the cycles are marked by an increase in lake level, surface
271 motion and SO₂ flux, Oppenheimer et al. (2009) and Boichu et al. (2010) suggested that they
272 are associated with the arrival of foaming magma batches in the lava lake (still exsolving
273 water at near atmospheric pressure). We now observe that the “top” of the cycle is
274 consistently associated with significantly more oxidized conditions ($\log fO_2 = \text{QFM} - 0.65$) than
275 the “bottom” of the cycles ($\log fO_2 = \text{QFM} - 1.16$). If the “top” of the cycles is indeed
276 associated with the influx of rising magma batches, then these batches appear to be releasing
277 gas whose composition is a relic of chemical equilibrium acquired at some depth. This
278 signature may be preserved as a result of rapid ascent of the magma batch (i.e., fast with
279 respect to the kinetics of redox reactions such as [1] and [2]). The dichotomy we identify
280 between the oxidized “top” and reduced “bottom” of the cycles therefore provides further
281 empirical evidence for redox stratification in the Erebus plumbing system as discussed in
282 Oppenheimer et al. (2011) and Burgisser et al. (in review), and as hypothesized from a more
283 general standpoint by Burgisser and Scaillet (2007).

284

285 *Conclusion*

286 In-situ measurements of the gas plume emitted from the lava lake of Erebus volcano by means
287 of a multi-gas sensing instrument indicate that the hydrogen abundance in the magmatic gas
288 phase is around 1.6 mol%. These measurements constrain the oxidation state of the lava lake
289 to $\sim \text{QFM} - 0.9$ log units, consistent with previous estimates; provide strong evidence that
290 hydrogen burning is not prevalent at the surface of the lake; and that hydrogen is at least

291 largely kinetically inert in the gas/aerosol plume rising in the crater. The hydrogen flux to the
292 atmosphere from the summit of Erebus is estimated at 2.8 Mg d⁻¹. A strong ~10 min
293 periodicity in the proportions of H₂ and other species in the plume infers corresponding redox
294 state variations, and points to a pulsatory supply of magma to the top of the lava lake. The
295 more oxidized signature of the magma periodically entering the lake provides strong
296 empirical evidence of a redox stratification in the shallow plumbing system, as has been
297 hypothesized by previous numerical models.

298

299 *Acknowledgments*

300 This research was supported by grant ANT-0838817 from the Office of Polar Programs
301 (National Science Foundation), and grant 202844 (« DEMONS ») from the European
302 Research Council (FP7). YM was additionally supported by the University of Cambridge
303 Home and EU Scholarship Scheme. We thank Tehnuka Ilanko, Bill McIntosh, Nial Peters and
304 Aaron Curtis for assistance in the field.

305 *References*

- 306 Aiuppa A, Bertagnini A, Métrich N, Moretti R, Di Muro A, Liuzzo M, Tamburello G (2010)
307 A model of degassing for Stromboli volcano. Earth and Planetary Science Letters
308 295:195-204. doi:10.1016/j.epsl.2010.03.040.
- 309 Aiuppa A, Burton M, Caltabiano T, Giudice G, Guerrieri S, Liuzzo M, Murè F, Salerno G
310 (2010) Unusually large magmatic CO₂ gas emissions prior to a basaltic paroxysm.
311 Geophys Res Lett 37. doi:10.1029/2010GL043837.

- 312 Aiuppa A, Federico C, Giudice G, Gurrieri S, Valenza M (2006) Hydrothermal buffering of
313 the SO₂/H₂S ratio in volcanic gases: Evidence from La Fossa Crater fumarolic field,
314 Vulcano Island. *Geophys Res Lett* 33:5 PP. doi:200610.1029/2006GL027730.
- 315 Aiuppa A, Federico C, Giudice G, Gurrieri S (2005) Chemical mapping of a fumarolic field:
316 La Fossa Crater, Vulcano Island (Aeolian Islands, Italy). *Geophys Res Lett* 32:4 PP.
317 doi:200510.1029/2005GL023207.
- 318 Aiuppa A, Shinohara H, Tamburello G, Giudice G, Liuzzo M, Moretti R (2011) Hydrogen in
319 the gas plume of an open-vent volcano, Mount Etna, Italy. *J Geophys Res* 116:8 PP.
320 doi:201110.1029/2011JB008461.
- 321 Aster R, Mah S, Kyle P, McIntosh W, Dunbar N, Johnson J, Ruiz M, McNamara S (2003)
322 Very long period oscillations of Mount Erebus Volcano. *J Geophys Res* 108.
323 doi:10.1029/2002JB002101.
- 324 Boichu M, Oppenheimer C, Tsanev V, Kyle P. (2010) High temporal resolution SO₂ flux
325 measurements at Erebus volcano, Antarctica. *Journal of Volcanology and Geothermal*
326 *Research* 190:325-336. doi:10.1016/j.jvolgeores.2009.11.020.
- 327 Burgisser A, Scaillet B (2007) Redox evolution of a degassing magma rising to the surface.
328 *Nature* 445:194-197.
- 329 Cruikshank DP, Morrison D, Lennon K (1973) Volcanic Gases: Hydrogen Burning at Kilauea
330 Volcano, Hawaii. *Science* 182:277 -279. doi:10.1126/science.182.4109.277.
- 331 Dibble RR, Kyle PR, Rowe CA (2008) Video and seismic observations of Strombolian
332 eruptions at Erebus volcano, Antarctica. *Journal of Volcanology and Geothermal*
333 *Research* 177:619-634.

- 334 Ilyinskaya E, Oppenheimer C, Mather TA, Martin RS, Kyle PR (2010) Size-resolved
335 chemical composition of aerosol emitted by Erebus volcano, Antarctica. *Geochem*
336 *Geophys Geosyst* 11. doi:10.1029/2009GC002855.
- 337 Johnson JW, Oelkers EH, Helgeson HC (1992) SUPCRT92: A software package for
338 calculating the standard molal thermodynamic properties of minerals, gases, aqueous
339 species, and reactions from 1 to 5000 bar and 0 to 1000°C. *Computers & Geosciences*
340 18:899-947. doi:16/0098-3004(92)90029-Q.
- 341 Kelly PJ, Kyle PR, Dunbar NW, Sims KWW (2008) Geochemistry and mineralogy of the
342 phonolite lava lake, Erebus volcano, Antarctica: 1972-2004 and comparison with older
343 lavas. *Journal of Volcanology and Geothermal Research* 177:589-605.
- 344 Martin RS, Roberts TJ, Mather TA, Pyle DM (2009) The implications of H₂S and H₂ kinetic
345 stability in high-T mixtures of magmatic and atmospheric gases for the production of
346 oxidized trace species (e.g., BrO and NO_x). *Chemical Geology* 263:143-150.
347 doi:16/j.chemgeo.2008.12.028.
- 348 Novelli PC, Lang PM, Masarie KA, Hurst DF, Myers R, Elkins JW (1999) Molecular
349 hydrogen in the troposphere: Global distribution and budget. *J Geophys Res* 104:444.
- 350 Oppenheimer C (2010) Ultraviolet Sensing of Volcanic Sulfur Emissions. *ELEMENTS* 6:87-
351 92. doi:<p>10.2113/gselements.6.2.87</p>.
- 352 Oppenheimer C, Kyle PR (2008) Probing the magma plumbing of Erebus volcano, Antarctica,
353 by open-path FTIR spectroscopy of gas emissions. *Journal of Volcanology and*
354 *Geothermal Research* 177:743-754.

- 355 Oppenheimer C, Kyle PR, Tsanev VI, McGonigle AJS, Mather TA, Sweeney D (2005) Mt.
356 Erebus, the largest point source of NO₂ in Antarctica. *Atmospheric Environment*
357 39:6000-6006. doi:16/j.atmosenv.2005.06.036.
- 358 Oppenheimer C, Lomakina AS, Kyle PR, Kingsbury NG, Boichu M (2009) Pulsatory magma
359 supply to a phonolite lava lake. *Earth and Planetary Science Letters* 284:392-398.
- 360 Oppenheimer C, Moretti R, Kyle PR, Eschenbacher A, Lowenstern JB, Hervig RL, Dunbar
361 NW (2011) Mantle to surface degassing of alkalic magmas at Erebus volcano,
362 Antarctica. *Earth Planet Sci Lett* 306:261-271. doi:10.1016/j.epsl.2011.04.005.
- 363 Oppenheimer C, Fischer TP, Scaillet B (in press) Volcanic degassing: process and impact.
364 *Treatise on Geochemistry*.
- 365 Shinohara H (2005) A new technique to estimate volcanic gas composition: plume
366 measurements with a portable multi-sensor system. *Journal of Volcanology and*
367 *Geothermal Research* 143:319-333. doi:16/j.jvolgeores.2004.12.004.
- 368 Sweeney D, Kyle PR, Oppenheimer C (2008) Sulfur dioxide emissions and degassing
369 behavior of Erebus volcano, Antarctica. *Journal of Volcanology and Geothermal*
370 *Research* 177:725-733. doi:16/j.jvolgeores.2008.01.024.
- 371 De Vito S, Massera E, Quercia L, Di Francia G (2007) Analysis of volcanic gases by means
372 of electronic nose. *Sensors and Actuators B: Chemical* 127:36-41.
373 doi:16/j.snb.2007.07.042.
- 374 Zreda-Gostynska G, Kyle P., Finnegan D, Prestbo K. (1997) Volcanic gas emissions from
375 Mount Erebus and their impact on the Antarctic environment. *J Geophys Res* 102:055.
376

377 **Tables**

378 **Table 1:** Estimated composition of the Erebus plume in mol% and in molar ratio. The
379 CO₂/CO and SO₂/H₂O molar ratios are obtained from Oppenheimer et al. (2009). The H₂/SO₂
380 and CO₂/SO₂ molar ratios are obtained from the “MultiGas” instrument measurements and the
381 SO₂/H₂S molar ratio is calculated using the “Dcompress” software from Burgisser et al (in
382 review). The “Top of cycle” composition correspond to the “mixed plume” composition of
383 Oppenheimer et al. (2009) while the “Bottom of cycle” composition correspond to the
384 “conduit gas” composition of Oppenheimer et al. (2009).

385

386 **Figures**

387 **Figure 1: a)** Typical field operating conditions of the Licor 840 and multigas sensor at the
388 crater rim. Gases are pumped through both instruments via a narrow hose connected to a
389 particle filter to avoid contamination of the instrument. **b)** View of Erebus (looking north)
390 under optimal plume sampling conditions on 26 December 2010. Turbulent airflow results in
391 grounding of the plume allowing for easy sampling.

392

393 **Figure 2:** Example of time series for gas mixing ratios obtained from both instruments (the
394 multi-gas sensor and LI-840). This 1-h-long time series is an extract from a 10-h-long run
395 acquired at the crater rim on 27 December 2010. All gas species are reported in ppmv.

396

397 **Figure 3: a)** Hydrogen time series (red) and aligned time series (corrected for instrumental
398 offset between sensors) of the estimated hydrogen counts from cross sensitivity with CO gas
399 (in blue) estimated as 4% of the CO₂ signal from which a constant background atmospheric
400 value of 387.5 ppmv is subtracted and whose residual is divided by 13 (from measured

401 CO₂/CO ratio in Oppenheimer et al. 2009). The dotted black line represents the residual of the
402 H₂ time series after removal of the H₂ counts due to CO cross-sensitivity. b) H₂ and SO₂ time
403 series after correction of H₂ from atmospheric background concentration and CO cross-
404 sensitivity and after alignment of both times series from correction of an offset calculated
405 using the maximum correlation factor between the time series.

406

407 **Figure 4: A: H₂-SO₂ and B: CO₂-SO₂ Scatter plots from six days of sampling of the Erebus**
408 **plume under favourable conditions a) 26 December 2010, data recorded from 11:20 to 16:33 h**
409 **UTC. b) 28 December 2010, data recorded from 02h16 to 10h01 UT. c) December 29th 2010,**
410 **data recorded from 11h07 to 13h58 UT. d) December 30th 2010, data recorded from 06h25 to**
411 **11h45 UT. e) December 31st 2010, data recorded from 04h10 to 06h12 UT. f) January 03rd**
412 **2011, data recorded from 22h42 to 01h32 UT. Regression lines are shown in red and**
413 **corresponding parameters displayed on the lower right corner of each plot.**

414

415 **Figure 5: Morlet Wavelet transform pseudo-periodogram computed from a 3 h time series of**
416 **the H₂/SO₂ ratio obtained from a 10 h long run of the MultiGas instrument on 3 January 2011.**
417 **Note the strong transform modulus emerging steadily at a period of ~10 min. The central**
418 **diagrams shows a 3 h time series of the evolution of the H₂/SO₂ ratio in which ~10 min cycles**
419 **(600 sec) can be observed. The lower diagram shows the evolution of the SO₂/H₂ and**
420 **SO₂/CO₂ ratios for the first 1400 sec (~23min) of a time series obtained from an 8 h long run**
421 **of the MultiGas instrument on 26 December 2010. This lower diagram shows 3 cycles of ~8**
422 **min each.**

423

Table 1

	Mean	mol%	
		Top of cycle	Bottom of cycle
CO ₂	44.00	34.86	47.25
H ₂ O	47.84	57.62	43.37
SO ₂	1.10	1.39	0.94
CO	3.30	2.61	3.54
HCl	0.46	0.56	0.42
HF	1.16	1.39	1.05
H ₂	1.58	1.39	1.89
OCS	0.01	0.01	0.01
H ₂ S	0.55	0.16	1.53
		mol/mol	
CO ₂ /CO	13.33	13.33	13.33
SO ₂ /H ₂ O	0.02	0.02	0.02
H ₂ /SO ₂	1.44	1.00	2.00
CO ₂ /SO ₂	40.00	25.00	50.00
SO ₂ /H ₂ S	2.01	8.72	0.62
log(fO ₂) at 1000°C	-11.90	-11.63	-12.14
Delta QFM	-0.92	-0.65	-1.16

Moussallam et al., Table 1

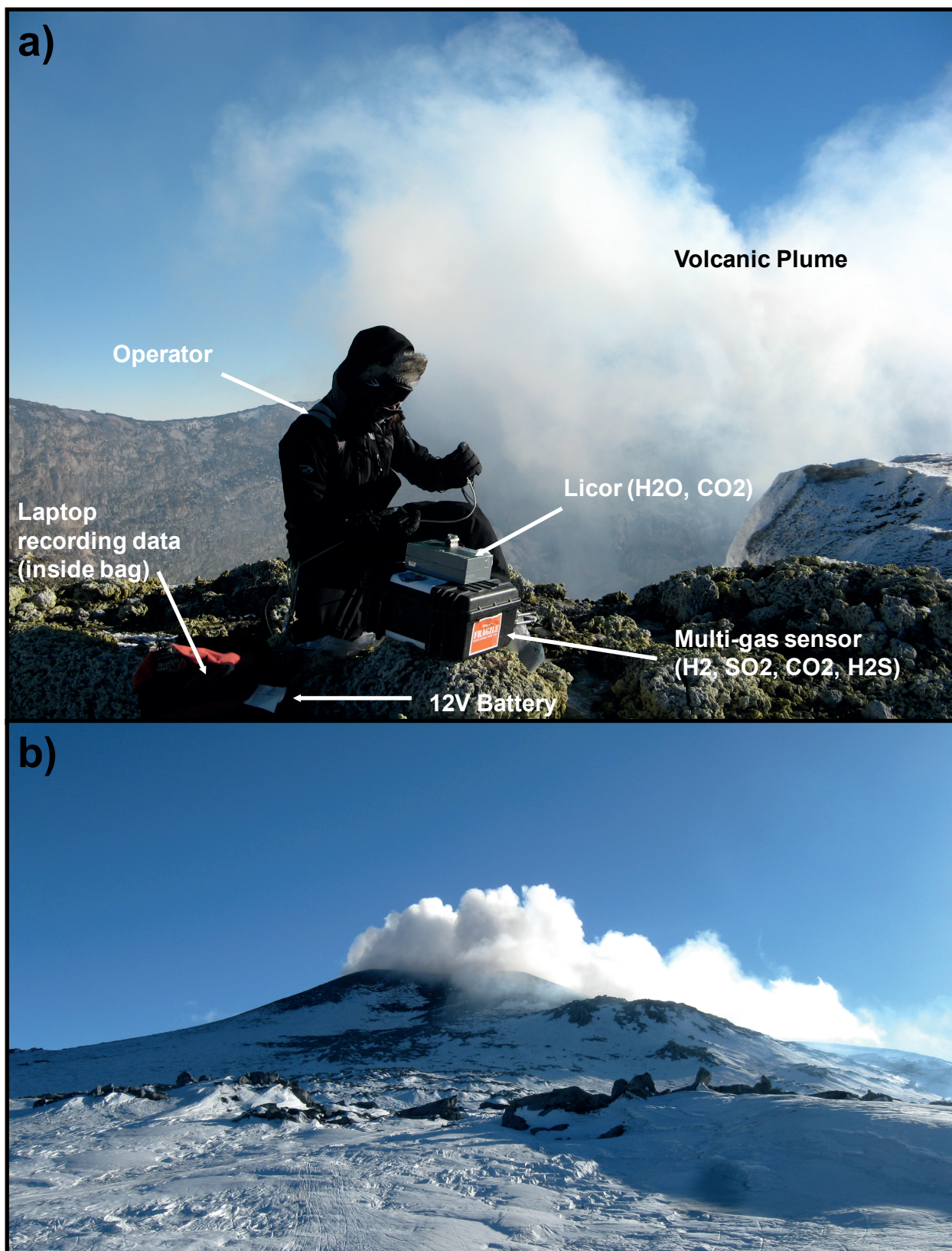


Figure 1 Moussallam et al.,

Figure 2

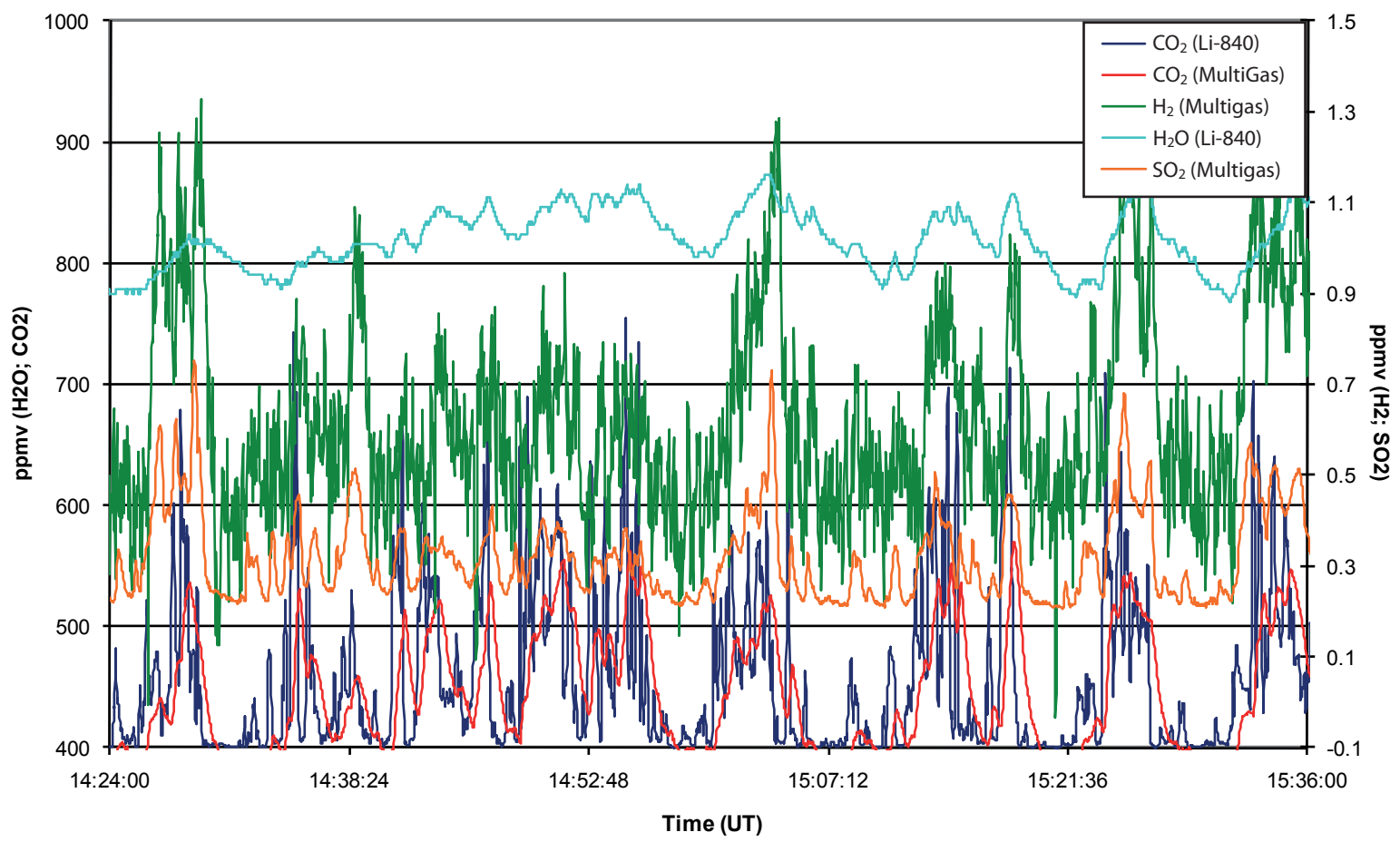


Figure 2 Moussallam et al.,

Figure 3

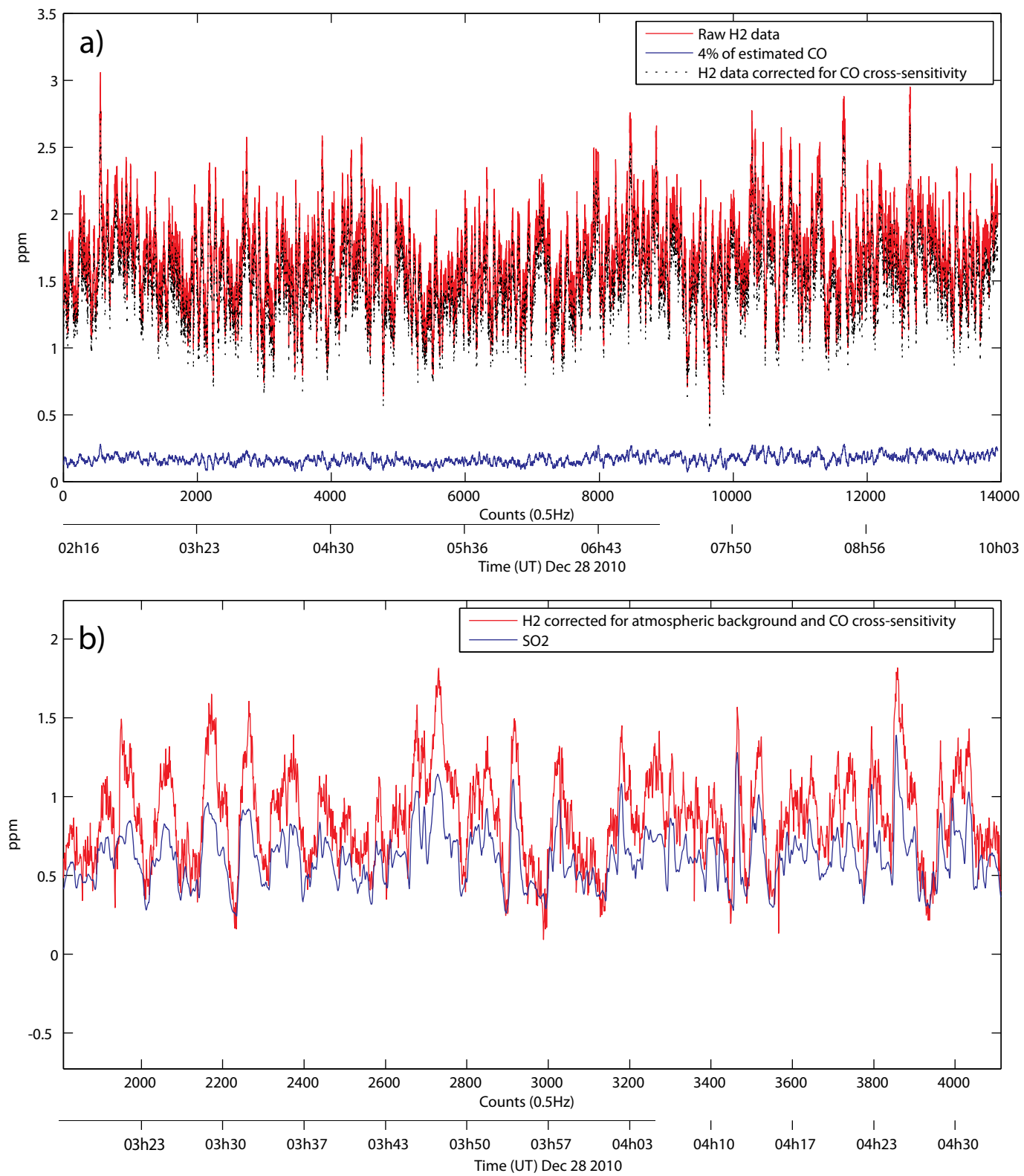


Figure 3 Moussallam et al.,

Figure 4a

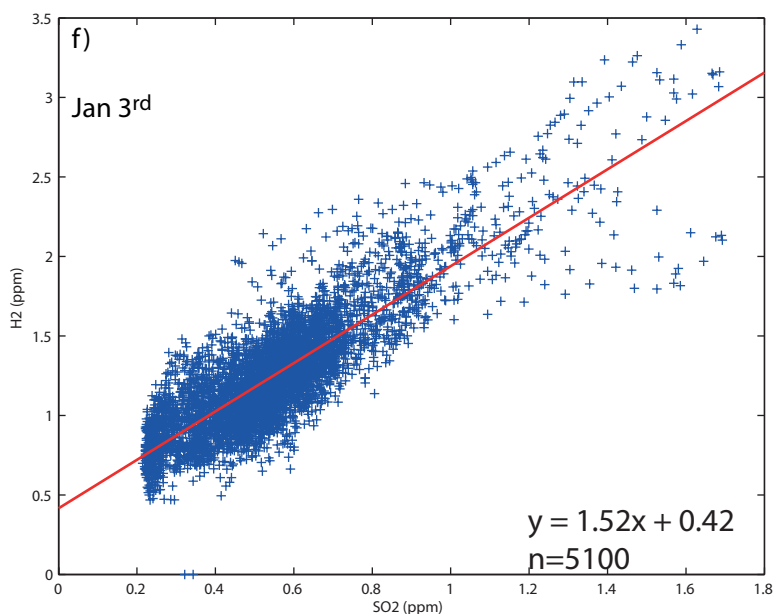
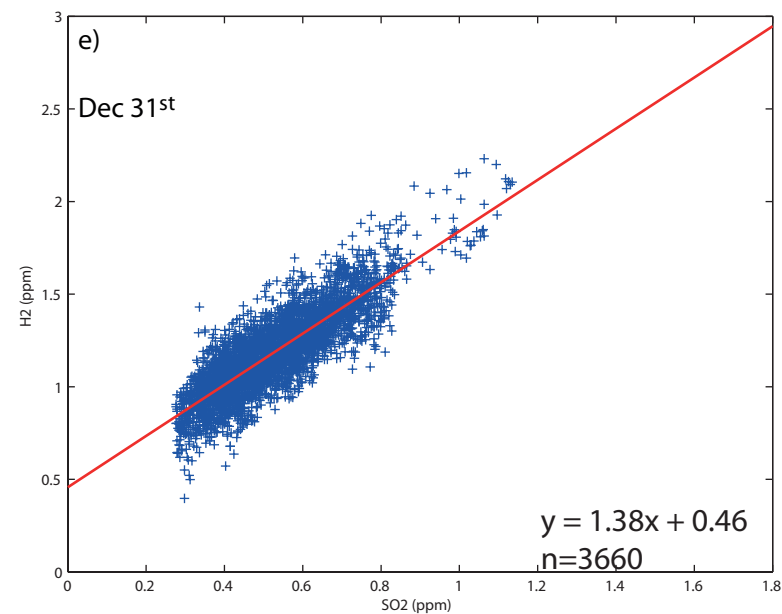
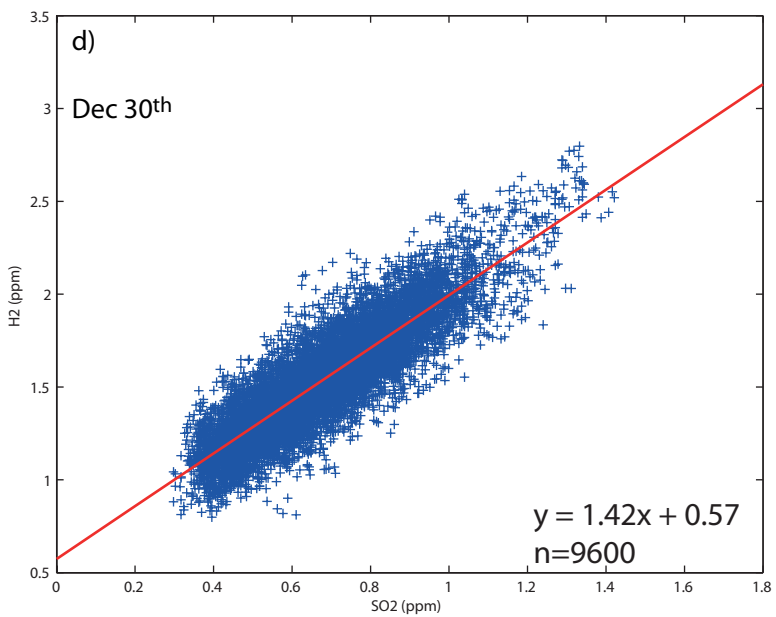
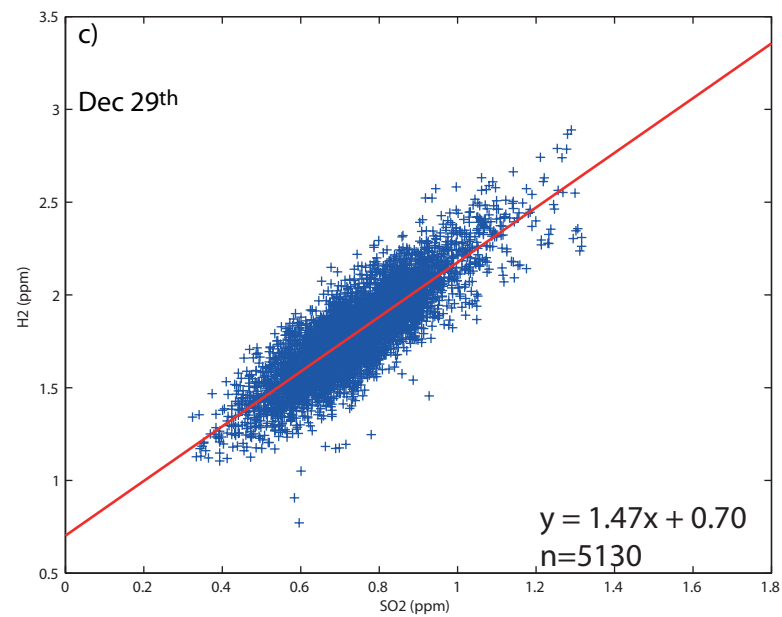
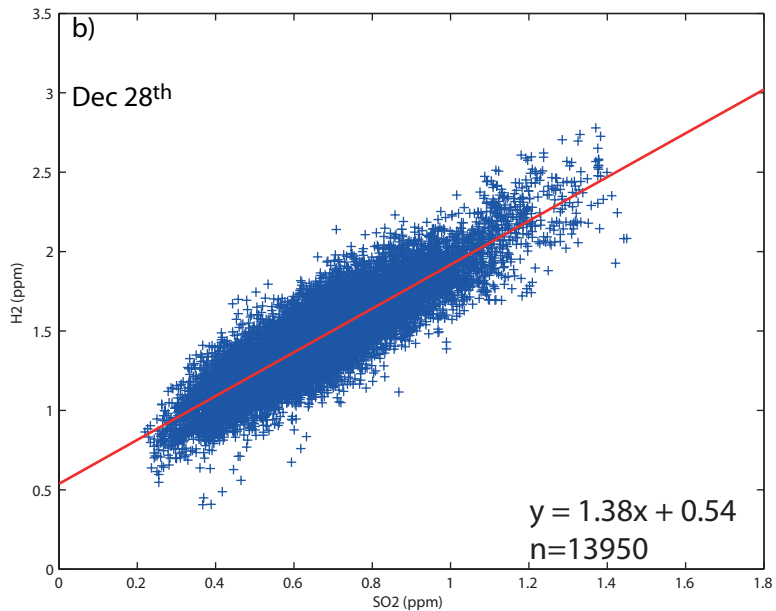
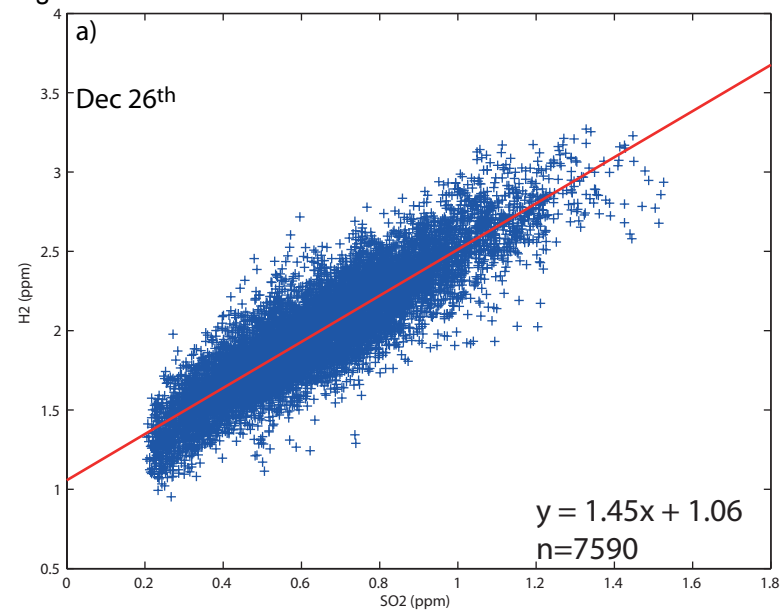


Figure 4 A Moussallam et al.,

Figure 4b

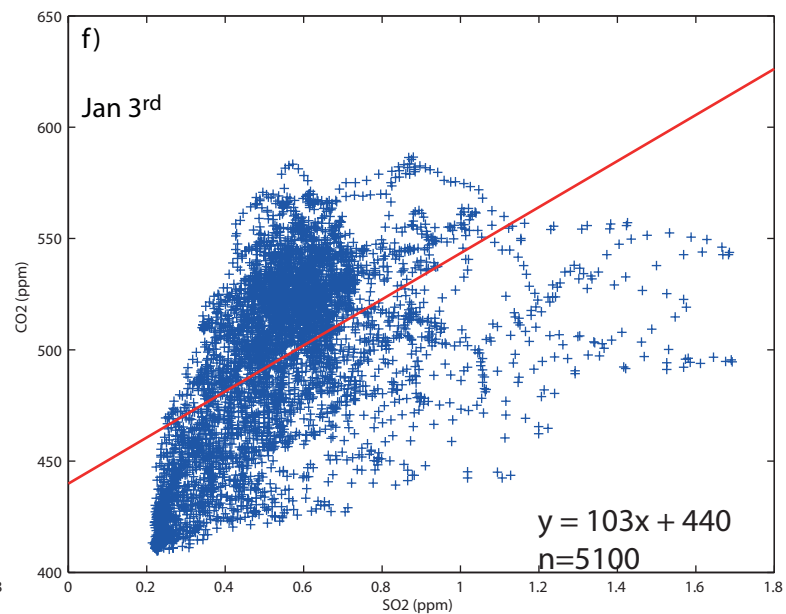
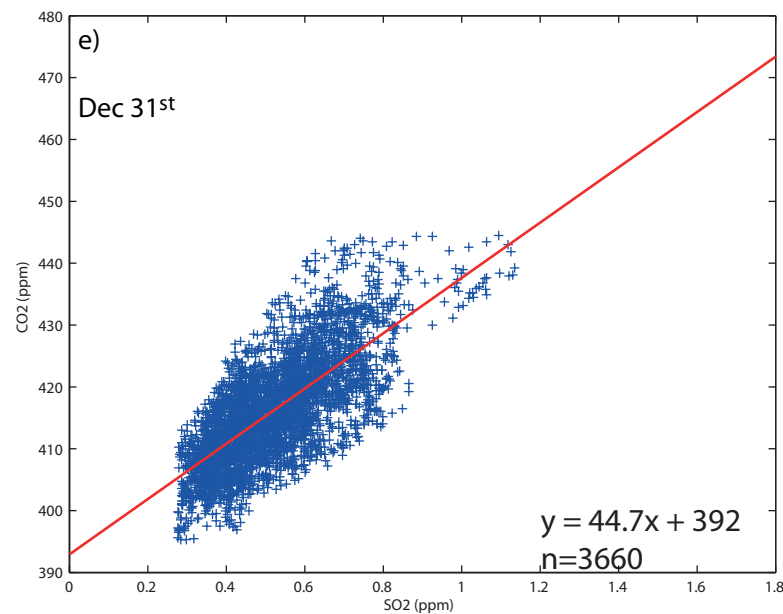
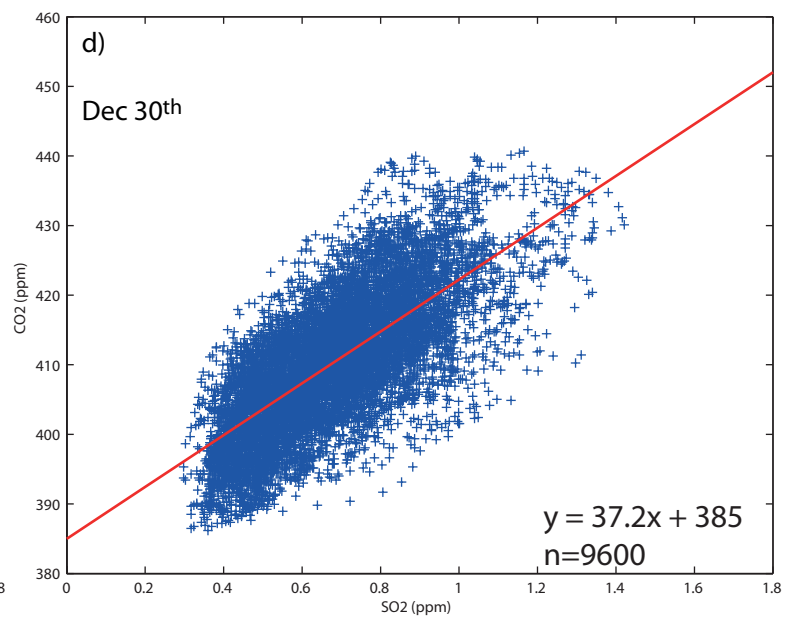
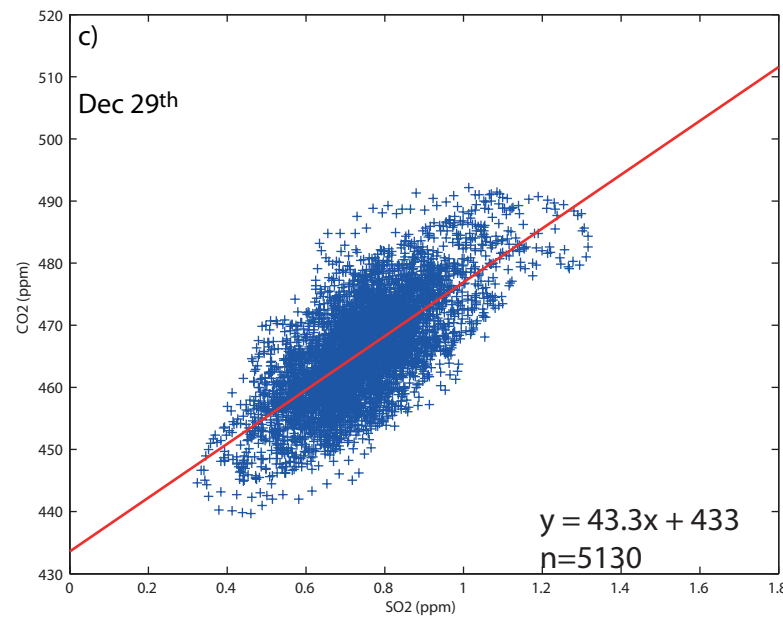
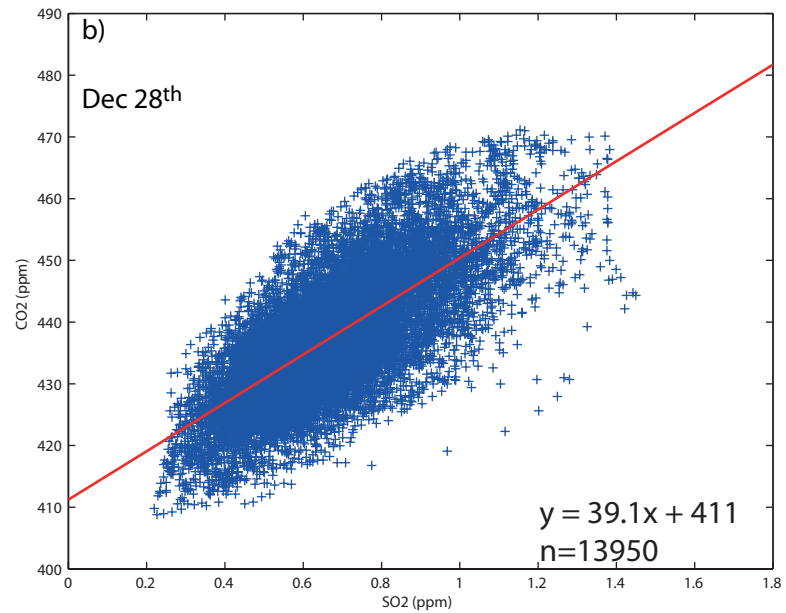
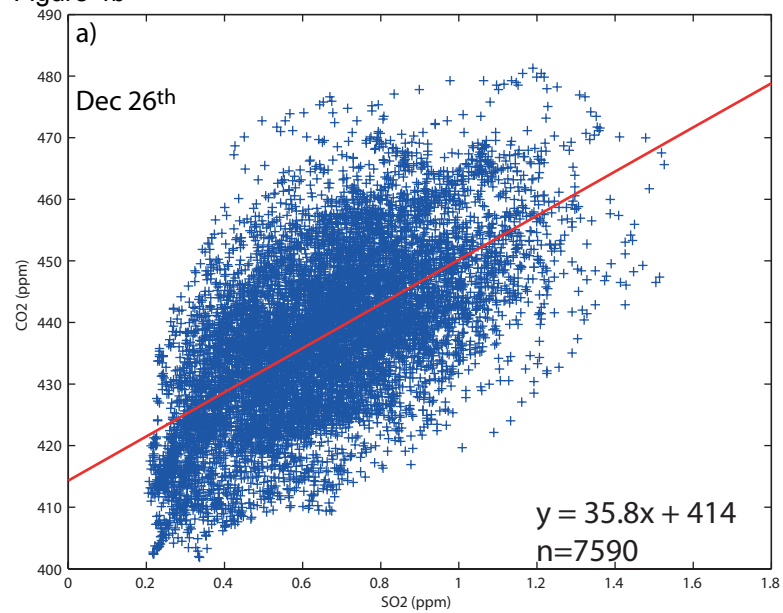


Figure 4 B Moussallam et al.,

Figure 5

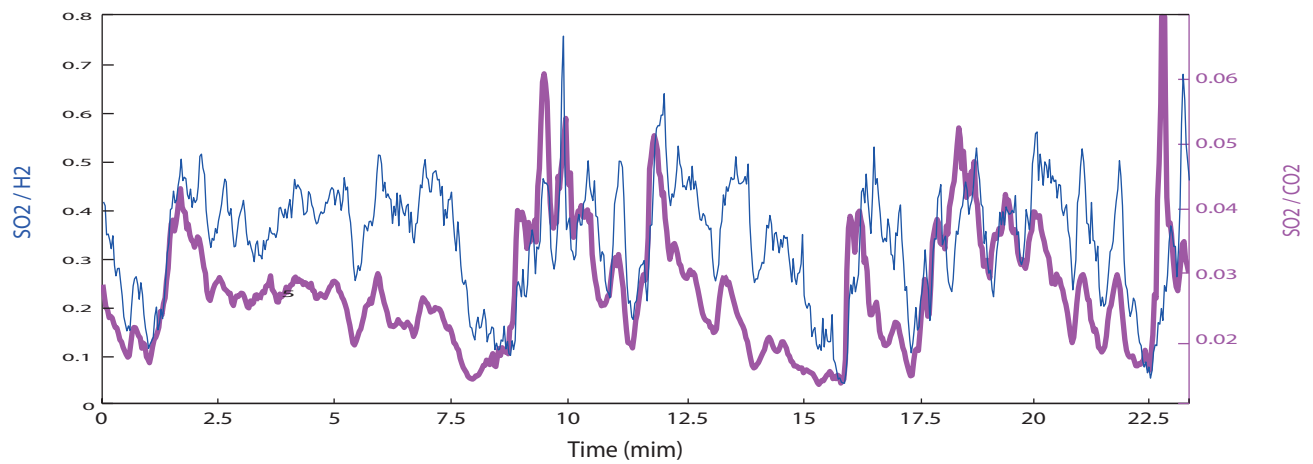
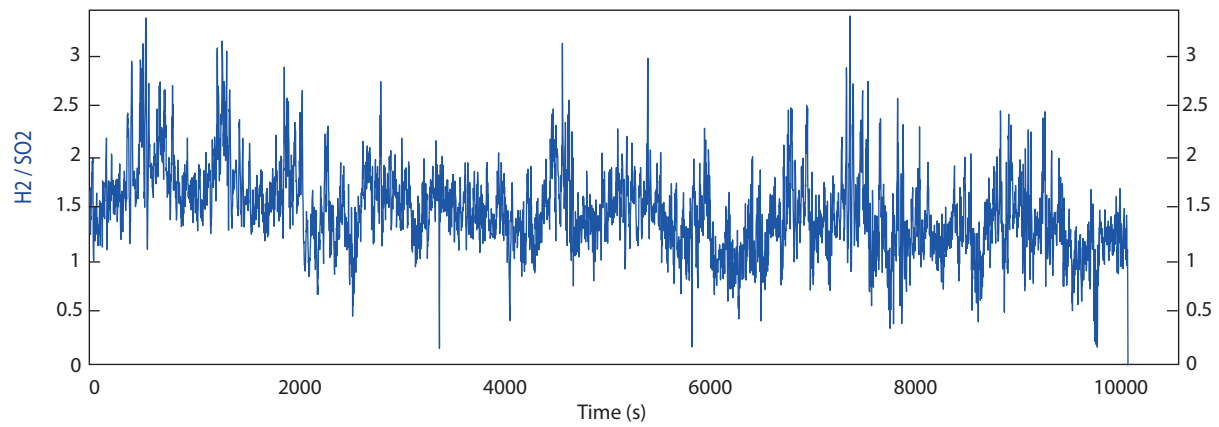
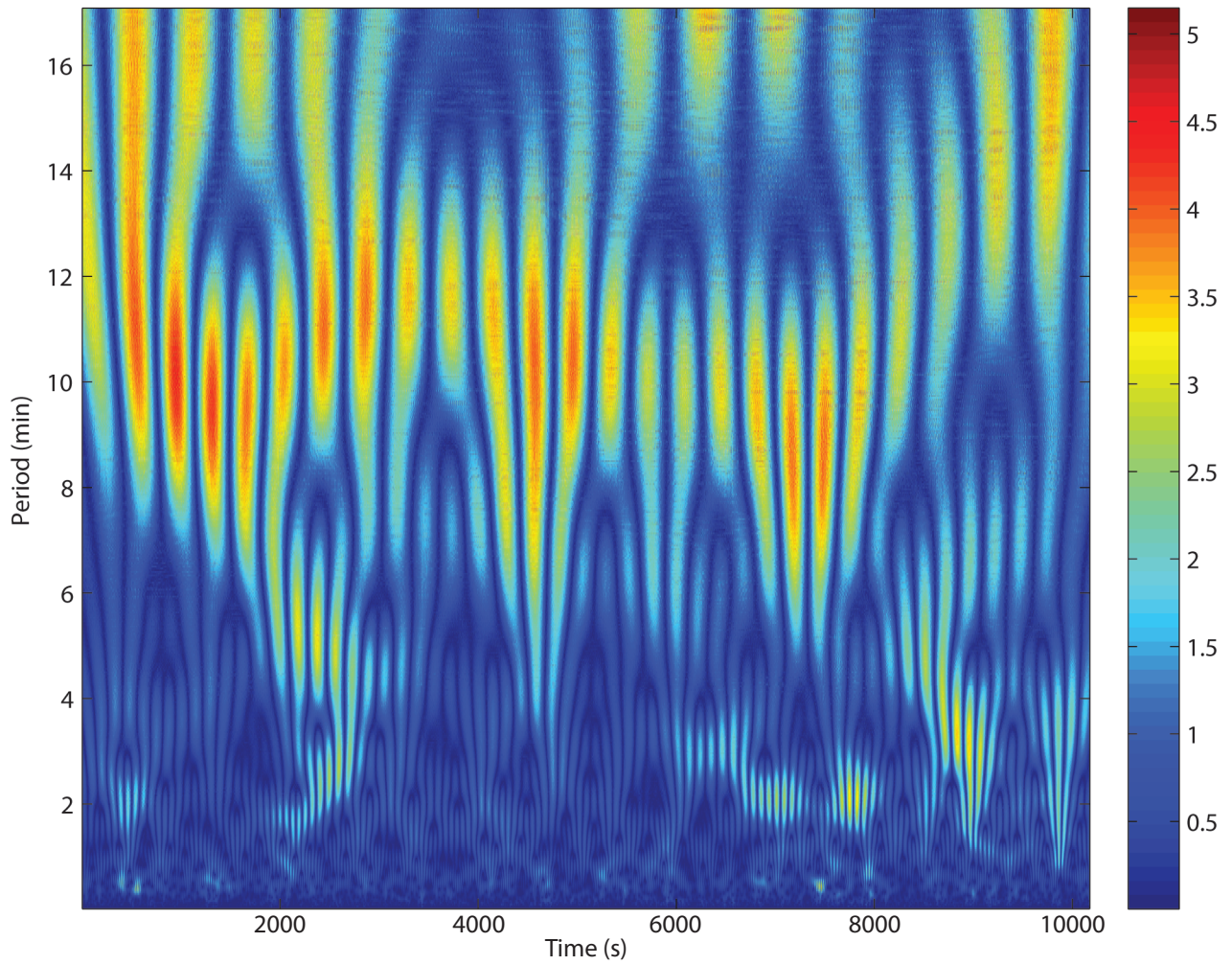


Figure 5 Moussallam et al.,